Spatial-frequency multiplication with multilevel interference lithography

Chih-Hao Chang,[a] Y. Zhao, R. K. Heilmann, and M. L. Schattenburg
Space Nanotechnology Laboratory, Massachusetts Institute of Technology, Cambridge, Massachusetts 02139

(Received 17 June 2008; accepted 4 August 2008; published 1 December 2008)

The authors present a large-area spatial-frequency multiplication fabrication process for patterning one-dimensional periodic structures using multilevel interference lithography. In this process, multiple grating levels with different phase offsets are overlaid by aligning to a reference grating. Each grating level is pattern transfered into a single hard mask layer, effectively reducing the grating period. The linewidth of the grating lines is controlled with nanometer repeatability by plasma etching and an image-reversal process. The authors demonstrate overlay accuracy of 0.6 ± 1.9 nm over 16×12 mm^2 for two levels of 200 nm period gratings. Using this process, a subdiffraction-limited resolution grating with 100 nm period is fabricated using light with $\lambda = 351.1$ nm. This process can also be used to fabricate more complex periodic geometries.
 [DOI: 10.1116/1.2976604]

I. INTRODUCTION

Periodic nanostructures have many interesting physical properties. Grating structures that are periodic in one dimension are used in various active research fields, including x-ray and extreme ultraviolet spectroscopy,[1–3] atom diffraction,[4] and templated self-assembly.[5] In many of these applications the functionality of the grating improves with smaller periodicity. It is therefore important to fabricate gratings with high spatial frequency.

Interference lithography (IL) is an effective technique for fabricating grating structures, as it provides relatively large exposure areas and high spatial-phase coherence. However, IL has limitations in its spatial resolution, and the finest period attainable is $\lambda/2n$, where λ is the light source wavelength and n is the refractive index of the medium. To fabricate gratings with sub-100-nm period, several approaches including the use of extreme ultraviolet sources[6,7] and immersion techniques have been reported.[8] However these methods require exotic light sources and expensive optical elements while the resulting grating areas are often small. Other process-based self-alignment techniques[9,10] are effective for spatial-frequency multiplication, but are less versatile in terms of pattern geometry.

In this article we explore an alternative fabrication process for spatial-frequency multiplication based on multiple exposures.[11] Our method aligns and overlays two levels of 200 nm period grating pattern with high accuracy to produce a large-area grating with 100 nm period. Key issues such as linewidth control and overlay accuracy are examined in detail. An image-reversal process was developed to fabricate high duty-cycle grating patterns with nanometer repeatability. Using this multilevel process, the wavelength-limited resolution of interference lithography can be extended by means of high precision metrology and well-controlled fabrication techniques. Furthermore, the method we describe is a general approach of overlaying multiple levels of periodic structures. Spatial-frequency multiplication is merely one application, and more complex geometries can be fabricated.

II. MULTILEVEL INTERFERENCE LITHOGRAPHY PROCESS

The multilevel IL process is illustrated in Fig. 1. Using a light source with $\lambda = 351.1$ nm, a reference grating with $p = 200$ nm is patterned and etched with reactive ion etching (RIE) into silicon nitride in the outer area of the substrate, shown in Fig. 1(a). The reference grating will then be used as a fiducial pattern for subsequent exposures of overlaid patterns.[12] The substrate is spincoated with antireflection coating (ARC) (Brewer Science i-CON-16) and resist (Sumitomo PFI-88A2), and the reference grating region is cleaned by oxygen plasma, as shown in Fig. 1(a). After aligning to the reference grating, the first grating level is exposed and developed with linewidth w. The pattern is etched with O_2 and CF_4 RIE into the ARC and nitride layers, respectively, as shown in Figs. 1(b) and 1(c). The process is then repeated to expose the second grating level with a π phase offset, shown in Figs. 1(d)–1(f). The final grating in nitride then has a resulting period $p/2 = 100$ nm.

This process presents a conceptually simple technique for spatial-frequency multiplication. This process can be further repeated for higher multiplication factors, depending on the duty-cycle w/p of each grating level. For example, duty cycles of 0.75 and 0.875 are needed for twofold and fourfold factors, respectively. An appealing advantage of this approach is that finer period gratings can be fabricated without needing to change the light source, optical components, or resist material.

The two key challenges that need to be addressed in order for this process to be successful are linewidth control and overlay accuracy. If there are significant overlay or linewidth errors, the fundamental spatial frequency will not be completely suppressed. To control the linewidth, we developed an image-reversal process with plasma trimming which allows the fabrication of high duty-cycle grating levels with

[a]Electronic mail: chichang@mit.edu

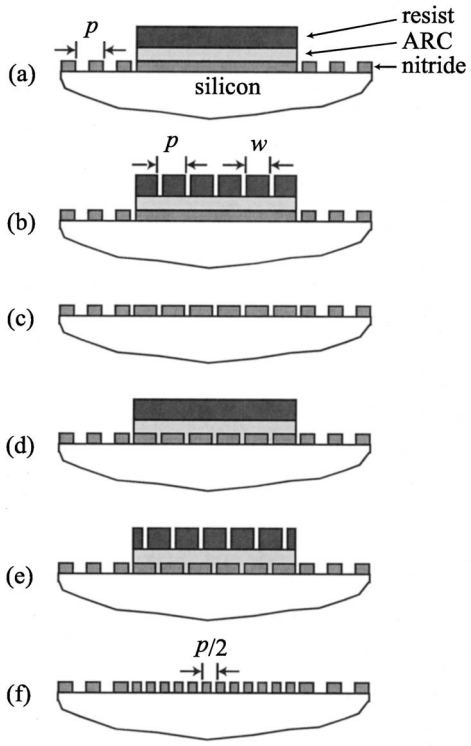

FIG. 1. Multilevel IL process starts by (a) patterning a reference grating at the periphery of the substrate with period p. The substrate is then spincoated with ARC and resist. (b) The first grating level is exposed after aligning to the reference grating. (c) The grating pattern is transfered into the nitride layer and the substrate is cleaned. (d) The substrate is spincoated with ARC and resist. (e) The second grating level is exposed at a π phase offset to the first exposure. (f) After transferring the pattern, the resulting pattern has period $p/2$.

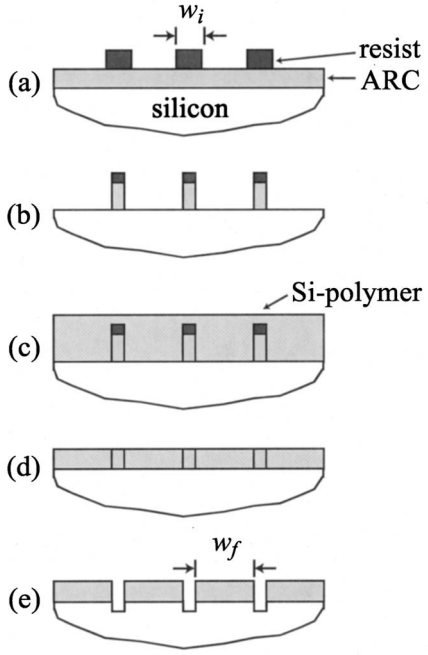

FIG. 2. Image-reversal process starts with (a) a positive resist grating over ARC with linewidth w_i. (b) The grating pattern is transfered into ARC and trimmed with high pressure oxygen PE. (c) A silicon-containing polymer is spin coated. (d) The ARC is then exposed with RIE etch back, and (e) the pattern is transfered into the substrate. The final linewidth has $w_f > w_i$.

nanometer repeatability. High overlay accuracy is achieved by using high precision optical metrology to align every grating level to the reference grating.

III. LINEWIDTH CONTROL

An image-reversal process was developed in conjunction with plasma etching (PE) to control the linewidth of each grating level. This process is illustrated in Fig. 2. The process starts with a positive resist grating over ARC with initial linewidth w_i, as shown in Fig. 2(a). After transferring the pattern into ARC with O_2 RIE, the linewidth is reduced with high pressure oxygen PE, as shown in Fig. 2(b). The grating is then spincoated and planarized with a silicon-containing polymer (Molecular Imprints SILSPIN), as shown in Fig. 2(c). The ARC grating is then uncovered by CF_4 etch back and cleared using O_2 RIE, as shown in Figs. 2(d) and 2(e). The final grating pattern with linewidth $w_f > w_i$ is then etched into the substrate. Using this process, a high duty-cycle gratings can be fabricated with positive resist, which avoids process control problems posed by negative resists.

The PE trimming step in this process, depicted in Fig. 2(b), is the key to controlling the linewidth. The purpose of this step is to reduce the linewidth to a precise target, so that the final duty cycle after the image-reversal steps will be high. The effect of PE trimming is demonstrated in the cross-sectional scanning electron microscopy (SEM) image shown in the insets of Fig. 3, as the linewidth is reduced from 45 to 24 nm following a 90 s O_2 etch at 50 W and 0.1 Torr. To examine the PE trim rate, an experiment of linewidth versus etch time was conducted, with the results plotted in Fig. 3. The results show that the etch rate is fairly constant, as the data agree well with a linear fit. The linear dependence of linewidth on etch time demonstrates that PE trimming is an effective and precise method to control linewidth.

To determine the PE trim time, top-view SEM is used to measure the linewidth. Multiple SEM metrology and PE trim iterations can be used to ensure tight linewidth control. The approach is illustrated in Fig. 4. The initial linewidth after

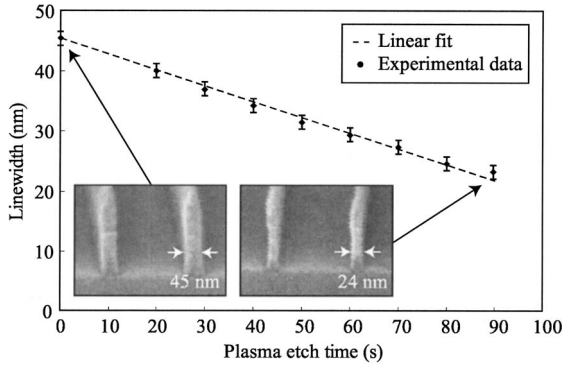

FIG. 3. Linewidth as a function of plasma etch time. The line is a linear fit to the experimental data.

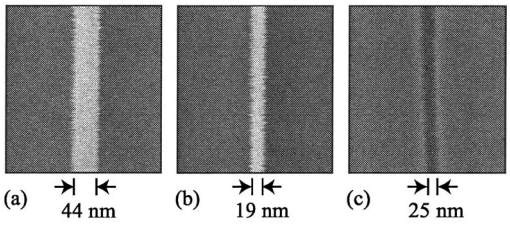

FIG. 4. Top-view SEM images of a grating line after (a) lithography, and (b) PE trim step. (c) Micrograph of the image-reversed trench etched into the substrate.

lithography is 44 nm, shown in Fig. 4(a). After the PE trim step, the linewidth has been reduced to 19 nm, shown in Fig. 4(b). The thin grating lines are then image reversed, resulting in a 25 nm wide trench, as shown in Fig. 4(c). Note that the image-reversal process does not perfectly reverse the tone of the grating pattern, and a linewidth increase of 6 nm has been observed in this experiment. However, the process is repeatable to a few nanometers, and the key is to trim the lines with PE to the same linewidth for every grating level. This image-reversal process with PE trimming has been used to fabricate ~0.88 duty-cycle grating levels with nanometer repeatability.

IV. OVERLAY ACCURACY

The other key challenge is the ability to align grating levels with high accuracy. To ensure accurate overlay, the phase of the reference grating is measured before exposure of each grating level by a grating interferometer. In this configuration, two beams satisfying the Littrow condition are used, so that the zeroth reflected order of the left beam and backdiffracted first order of the right beam copropagate. The two beams interfere and provide an intensity signal, which is measured by a detector to determine the relative phase of the reference grating. By changing the frequencies of the two incident beams, both homodyne and heterodyne[13] phase detection are used. This alignment method has been implemented using the MIT Nanoruler,[14,15] and overlay accuracy of -1 ± 2.8 nm (1σ) between two 574 nm period gratings over 35×25 mm^2 area has been achieved.[16]

The overlay accuracy between two 200 nm period grating levels is analyzed. After the exposure of the second level, the overlay accuracy can be measured by top-view SEM, as shown in Fig. 5. In the image, the dark lines (A) are trenches etched into nitride from the first grating level and the bright lines (B) are resist patterned by the second grating level. For perfect overlay alignment, the two grating levels should be separated by 100 nm, which the SEM image closely demonstrates.

To examine large-area overlay accuracy, we imaged the sample 144 times over a 16×30 mm^2 area, with each image 2 mm apart from the next. Each micrograph then resembles the image, as depicted in Fig. 5. Using a maximum and minimum detection algorithm, the phase overlay accuracy map can be calculated and plotted, as shown in Fig. 6. The phase map illustrates high overall overlay accuracy, with no apparent systematic alignment errors. However, there are local particle-induced distortions[17] by the vacuum chuck in the center region. For the area $x < 12$ mm, the overlay accuracy is 0.6 ± 1.9 nm (1σ) over a 16×12 mm^2 area.

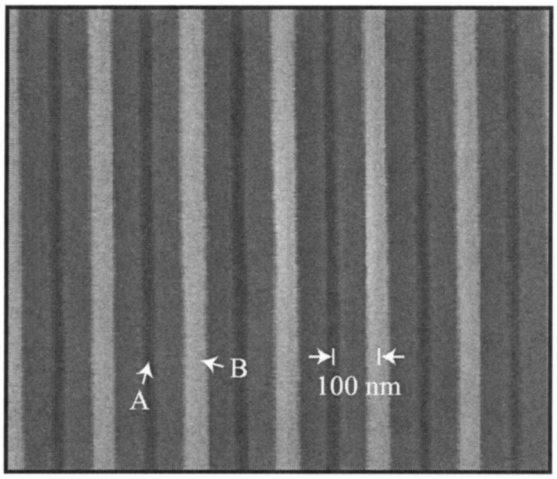

FIG. 5. Top-view SEM image of two overlaid 200 nm period grating levels. The dark lines (A) and bright lines (B) are the first grating level etched into nitride and the second grating level in resist, respectively.

V. RESULTS AND DISCUSSION

Using the multilevel IL process, a silicon nitride grating with 100 nm period was fabricated by overlaying two 200 nm period grating levels, shown in Fig. 7. In the image, even and odd number dark lines are trenches etched into the nitride layer patterned in two separate fabrication steps. The linewidth variation between the two levels cannot be visually detected. These results imply that the linewidth control is better than the spatial resolution of the SEM, which is around 1–2 nm.

These results are representative over the spatial-frequency doubled area of 16×30 mm^2, except for the areas with local particle-induced distortion. A visual confirmation of the successful suppression of the 200 nm period fundamental spatial frequency can be seen in Fig. 8, where the 100 mm diameter

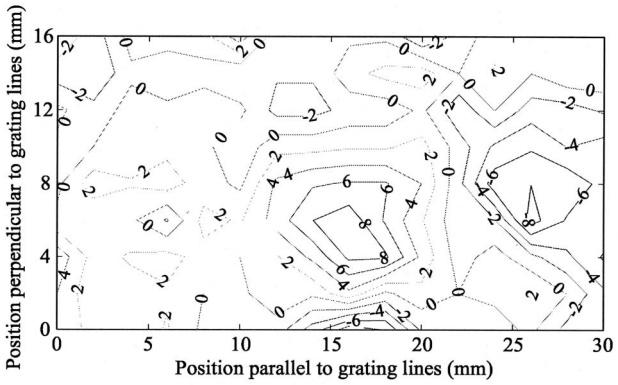

FIG. 6. Map of overlay error (nanometer) between two 200 nm period grating levels.

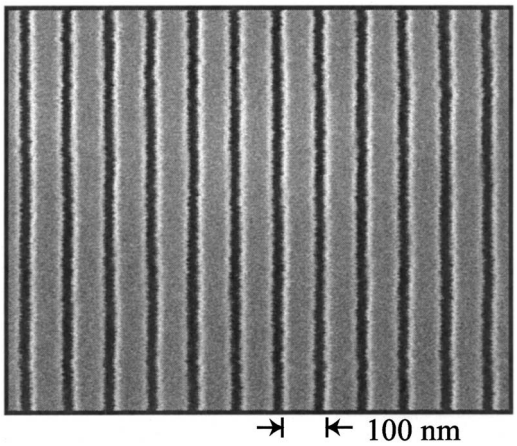

FIG. 7. Top-view SEM images of 100 nm period silicon nitride grating fabricated by overlaying two 200 nm period grating levels.

wafer sample is immersed in water. The dashed lines define the boundaries between the reference grating and spatial-frequency doubled areas. The two strips in between are shadowed areas that were not exposed. White light illuminates the sample at a shallow angle, and the immersion allows diffraction of blue wavelength from the 200 nm period reference grating, as shown in the picture. The grating period in the spatial-frequency doubled region, however, is subwavelength and no diffraction can be observed.

The multilevel IL process we have presented is a general scheme in which multiple levels of periodic nanostructures can be aligned and overlaid. Using this method, IL can evolve from the traditional limitation of single layer pattern.

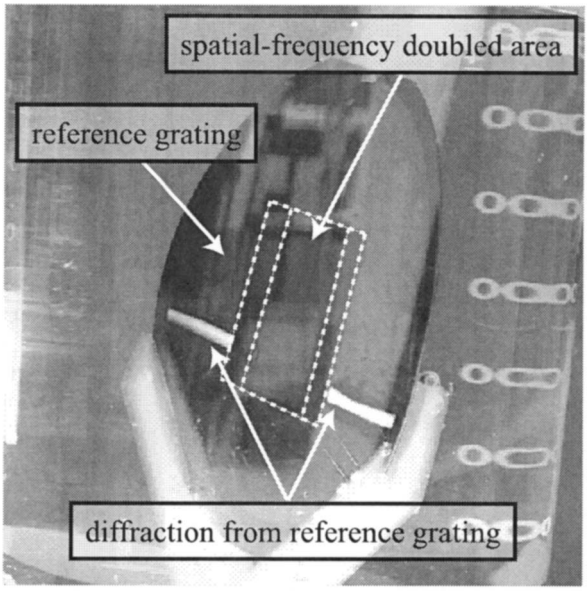

FIG. 8. Fabricated sample immersed in water and illuminated with a beam of white light to allow diffraction of blue wavelength from the 200 nm period reference grating. No diffraction can be observed from the spatial-frequency doubled grating.

By using multiple reference gratings, the multilevel approach described could also be used to fabricate phase-aligned two-dimensional patterns. These levels can then be stacked to fabricate complex three-dimensional structures such as photonic crystals.

VI. CONCLUSION

We have developed a large-area spatial-frequency multiplication process using multilevel IL. Two 200 nm period grating levels were aligned with π phase shift to a common reference grating to fabricate a silicon nitride grating with 100 nm period. An image-reversal process was used in conjunction with a PE trimming step to achieve a $\sim$0.88 duty-cycle grating pattern with nanometer repeatability. Using such high duty-cycle features, higher spatial-frequency multiplication factors can be obtained. The overlay accuracy of the two grating levels is measured to be 0.6 ± 1.9 nm (1σ) over a 16×12 mm^2 area. In principle, this process can be scaled to fabricate high-density gratings over 300 mm area.

ACKNOWLEDGMENTS

The authors gratefully acknowledge the outstanding technical assistance of Robert Fleming and Jim Daley. Student, staff, and facility support from the Space Nanotechnology Laboratory, NanoStructures Laboratory, Quantum Nanostructures and Nanofabrication Group, and Microsystems Technology Laboratory at MIT are also appreciated. This work was supported by the NASA Grant No. NNX07AG98G and the NSF Grant No. DMI-0506898.

[1] M. P. Kowalski, R. K. Heilmann, M. L. Schattenburg, C.-H. Chang, F. B. Berendse, and W. R. Hunter, Appl. Opt. **45**, 1676 (2006).
[2] J. F. Seely *et al.*, Appl. Opt. **45**, 1680 (2006).
[3] D. Hambach, G. Schneider, and E. M. Gullikson, Opt. Lett. **26**, 1200 (2001).
[4] D. W. Keith, M. L. Schattenburg, H. I. Smith, and D. E. Pritchard, Phys. Rev. Lett. **61**, 1580 (1988).
[5] J. Y. Cheng, C. A. Ross, E. L. Thomas, H. I. Smith, and G. J. Vancso, Appl. Phys. Lett. **81**, 3657 (2002).
[6] H. H. Solak, C. David, J. Gobrecht, V. Golovkina, F. Cerrina, S. O. Kim, and P. F. Nealey, Microelectron. Eng. **67–68**, 56 (2003).
[7] H. H. Solak, D. He, W. Li, S. Singh-Gasson, F. Cerrina, B. H. Sohn, X. M. Yang, and P. Nealey, Appl. Phys. Lett. **75**, 2328 (1999).
[8] T. M. Bloomstein, M. F. Marchant, S. Deneault, D. E. Hardy, and M. Rothschild, Opt. Express **14**, 6434 (2006).
[9] Z. Yu, W. Wu, L. Chen, and S. Y. Chou, J. Vac. Sci. Technol. B **19**, 2816 (2001).
[10] B. Cui, Z. Yu, H. Ge, and S. Y. Chou, Appl. Phys. Lett. **90**, 043118 (2007).
[11] S. R. J. Brueck, Proc. IEEE **93**, 1704 (2005).
[12] M. L. Schattenburg, C. Chen, P. N. Everett, J. Ferrera, P. Konkola, and H. I. Smith, J. Vac. Sci. Technol. B **17**, 2692 (1999).
[13] R. K. Heilmann, P. T. Konkola, C. G. Chen, G. S. Pati, and M. L. Schattenburg, J. Vac. Sci. Technol. B **19**, 2342 (2001).
[14] P. T. Konkola, C. G. Chen, R. K. Heilmann, C. Joo, J. C. Montoya, C.-H. Chang, and M. L. Schattenburg, J. Vac. Sci. Technol. B **21**, 3097 (2003).
[15] R. K. Heilmann, C. G. Chen, P. T. Konkola, and M. L. Schattenburg, Nanotechnology **15**, S504 (2004).
[16] Y. Zhao, C.-H. Chang, R. K. Heilmann, and M. L. Schattenburg, J. Vac. Sci. Technol. B **25**, 2439 (2007).
[17] P. T. Konkola, Ph.D. thesis, Massachusetts Institute of Technology, 2003.